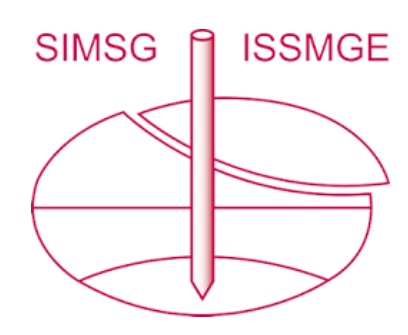
INTERNATIONAL SOCIETY FOR SOIL MECHANICS AND GEOTECHNICAL ENGINEERING



This paper was downloaded from the Online Library of the International Society for Soil Mechanics and Geotechnical Engineering (ISSMGE). The library is available here:

https://www.issmge.org/publications/online-library

This is an open-access database that archives thousands of papers published under the Auspices of the ISSMGE and maintained by the Innovation and Development Committee of ISSMGE.

The paper was published in the proceedings of the 7th International Conference on Earthquake Geotechnical Engineering and was edited by Francesco Silvestri, Nicola Moraci and Susanna Antonielli. The conference was held in Rome, Italy, 17 - 20 June 2019.

Seismic response of basal geogrid reinforced embankments supported over floating and end bearing piles

M. Radhika, M. Patel, B.R. Jayalekshmi & R. Shivashankar *National Institute of Technology Karnataka, Surathkal, India*

ABSTRACT: Embankments, roads and bridges are very important components of infrastructure. It is equally important that these structures are also able to resist earthquake forces and be functional at all times. Since the bridge rests on rigid deep foundations and the approaching embankments to the bridge on both sides could be resting on weak and compressible soil, the bridge and embankment junction always experiences differential settlement problems. To overcome these settlements, construction of approach embankments supported by pile foundations with basal geogrid reinforcement is a viable solution. Lot of studies are available in literature on the analysis of these geogrid reinforced pile supported embankments subjected to static loading conditions. Very few studies are available on geogrid reinforced pile supported embankments (GRPE's) subjected to seismic excitations. Hence in the present study, 3-dimensional finite element analysis of 3 m high embankment made of pulverized fuel ash having crest width of 20 m and side slope of 1V:1.5H resting on 28 m thick soft marine clay subjected to seismic loading is considered. The soft marine clay is provided with 300 mm diameter RC piles having 22 m, 24 m, 26 m(Floating piles) and 28 m (End bearing piles) lengths arranged in a square grid pattern with centre to centre spacing of three times the diameter of the pile. Geogrid with tensile modulus of 2500 kN/m is considered as basal reinforcement. Maximum vertical and horizontal displacements along the embankment, settlement reduction ratio, differential settlements at crest, vertical and horizontal displacements at toe are evaluated. The embankment resting over end bearing pile stabilized soft marine clay experiences less settlements, less toe horizontal displacements, less differential settlements, larger settlement reduction ratio than the embankment resting over floating pile stabilized soft marine clay.

1 INTRODUCTION

GRPE's are a reliable solution to construct roads over thick soft clay deposits, bridge approach roads, widening of existing roads in congested areas and high speed rail roads etc. Marston & Anderson (1913), Terzaghi (1943), Carlsson (1987), Hewlett & Randolph (1988) and many others give empirical relations for the load transfer mechanism in piled embankments subjected to static loading conditions and the same empirical relations are used in many GRPE's design codes.

In recent decades, many numerical studies, experiments and case studies are available to understand the load transfer mechanism and settlement analysis of these geogrid reinforced pile supported embankments subjected to static loading conditions (Han & Gabr (2002), Liu et al. (2007), Smith & Filz (2007), Wachman et al. (2010), Briançon & Simon (2012), Ariyarathne & Liyanapathirana (2014), Bhasi & Rajagopal (2014), Bhasi & Rajagopal, (2015), Liu et al. (2017), Shen et al. (2018).

Even though many studies are available on the seismic performance of pile foundations Ousta & Shahrour (2001), Wang & Yuan (2005)) very few studies are seen on the dynamic analysis of geogrid reinforced piled embankments. Such as Thach et al. (2013) and Han et al. (2014) analyzed GRPE's subjected to cyclic loading. Panah et al. (2015) and Wang et al. (2015) studied the seismic performance of reinforced rigid retaining walls using large-scale shaking table tests. Armstrong et al. (2013) performed dynamic centrifuge model tests to investigate pile-pinning effects for the

embankment resting over piles. Wang & Mei (2012) studied the seismic performance of micropile supported embankment. Since, lateral spreading, foundation pile failure, huge total and differential settlements are the adverse effects of earthquakes on these GRPE's, there is a need to understand the behavior of these GRPE's subjected to seismic excitations.

Hence in this paper seismic performance of basal geogrid reinforced floating/end bearing pile supported embankments are analyzed based on maximum vertical and horizontal displacements along the embankment, settlement reduction ratio, differential settlements at crest, toe vertical and horizontal displacements.

2 METHODOLOGY

2.1 Numerical analysis

A 3 m high embankment made of pulverized fuel ash (PFA) with 20 m crest width constructed over 28 m thick soft marine clay was considered for the time history analysis. Hard stratum exists below clay layer. The embankment geometry is shown in Figure 1.

2.2 Idealization of soil

The properties of PFA, surface fill (Liu et al. 2007), soft marine clay which exists in Cochin region (IRC:113-2013, Jose et al, 1988) and hard soil considered for the analysis are listed in Table 1. All the soils considered for the finite element analysis were modeled as Mohr-coulomb material model. This model defines yielding when the combination of pressure and shear stress reaches the cohesion of the material particles. Yielding occurs when the shear stress on any plane in the material reaches the given criterion:

$$\tau = c - \sigma_{\rm m} \tan \varphi \tag{1}$$

Where, τ is the shear stress, c is the cohesion, σ_m is the mean stress and φ is the angle of internal friction.

2.3 Idealization of pile foundation

Piles of length (L) 22 m, 24 m, 26 m (Floating piles) and 28 m (End bearing pile) having 300 mm diameter (D) and arranged in a 3D spaced square grid pattern were considered. Floating

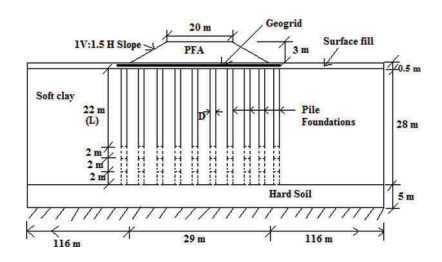


Figure 1. Details of embankment

Table 1. Soil Properties

Soil type	Unit Weight kN/m ³	Young's Modulus MN/m ²	Poisson's — ratio	Cohesion kN/m ²	Angle of internal friction	v _p m/s	$\frac{v_s}{m/s}$
PFA Surface fill	18.5 18.5	20	0.3 0.3	10 15	30 ⁰ 28 ⁰	119.5 70.7	63.9 37.8
Soft Marine clay Hard soil	14 21	4 250	0.45 0.3	12.5 50	20 40 ⁰	103.7	31.3 213.9

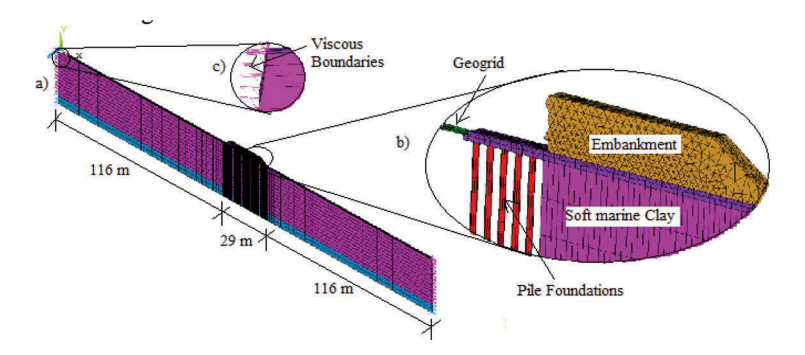


Figure 2. (a) A Slice of 3-Dimensional Finite element model of Embankment (b) Enlarged view of geogrid reinforced pile supported embankment(c)Enlarged view of viscous boundaries

pile length was considered based on the critical length of piles for the given site conditions (Satibi, 2009). Piles were modeled as linear elastic isotropic material with modulus of elasticity corresponding to M20 grade concrete, unit weight of 25 kN/m³ and Poisson's ratio of 0.15.

2.4 Idealization of geogrid reinforcement

For the 3 m high embankment considered, tensile strength design for the basal geogrid reinforcement was done according to BS8006. Based on the design, geogrid with tensile modulus of 2500 kN/m and Poisson's ratio of 0.3 with linear elastic isotropic material property was used as basal geogrid.

2.5 Modeling

Three-dimensional finite element modeling was performed using general purpose finite element software ANSYS. Both soil and piles were modeled using SOLID65 element. SOLID65 is an eight noded element with three degrees of freedom at each node: translations in the nodal x, y, and z directions. Geogrid was modeled using SHELL181 element with membrane effect. It is a four noded element with 3 translational degrees of freedom at each node. A slice of 3-dimensional finite element model of embankment, pile, geogrid and viscous boundaries are shown in Figure 2.

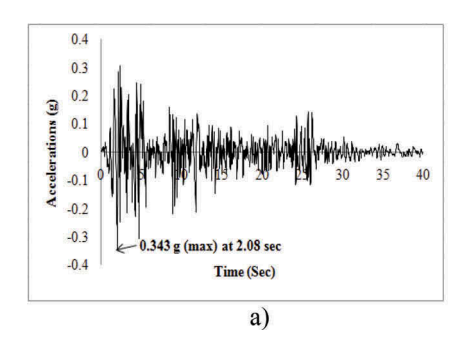
2.6 Boundary conditions

For time-history analysis, lateral boundary was taken at a distance of four times the base width of the embankment so that the waves propagated from the soil cannot reflect back (Ghosh and Wilson, 1969). To simulate the infinite soil medium, viscous boundaries were applied for the lateral boundaries using spring-damper element given by Kianoush and Ghaemmaghami, 2011. The equation of motion with additional damping matrix C* can be written as follows when the viscous boundaries are taken into account.

$$[M]\{\ddot{u}(t)\} + [C]\{\dot{u}(t)\} + [C^*]\{\dot{u}(t)\} + [K]\{u(t)\} = -[M]\{\ddot{u}_{\sigma}(t)\}$$
(2)

Where, [M] is the structural mass matrix, [C] is the structural damping matrix, [K] is the structural stiffness matrix, $\{\ddot{u}g(t)\}$ is the ground acceleration vector, $\{\ddot{u}(t)\}$ is the nodal acceleration vector, $\{\ddot{u}(t)\}$ is the nodal velocity vector, $\{u(t)\}$ is the nodal displacement vector and [C*] is the special damping matrix that is considered as follows,

$$[C^*] = \begin{bmatrix} A_n \rho \nu_p & 0 & 0\\ 0 & A_{t1} \rho \nu_s & 0\\ 0 & 0 & A_{t2} \rho \nu_s \end{bmatrix}$$
(3)



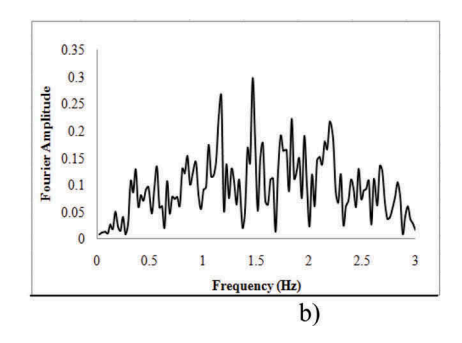


Figure 3. a) Acceleration time history of El Centro earthquake b) Fourier spectrum of El Centro earthquake

Where, v_p and v_s are the dilatational and shear wave velocity of the considered medium (Table 1), ρ is the density of soil medium, A_n , A_{t1} and A_{t2} are the fields controlling the viscous dampers and the subscripts n and t represent normal and tangential directions in the boundary.

2.7 Loading

To study the behavior of GRPE's under seismic excitations, time history record of El Centro earthquake (1940) was considered. It had a moment magnitude of 6.9 and was classified as intense earthquake. The peak acceleration was observed to be 0.34g. Only the horizontal component of El Centro earthquake acting transversely to the embankment was considered. The acceleration time history and Fourier spectrum of El Centro earthquake is shown in Figure 3.

3 RESULTS AND DISCUSSIONS

3.1 Natural frequency

The natural frequencies of GRPE's considered for the analysis with the corresponding Fourier amplitudes of the frequency content in El Centro earthquake are listed in Table 2.

3.2 Maximum vertical and horizontal displacements in the embankment

The maximum vertical and horizontal displacements in the embankment subjected to El Centro earthquake excitations are shown in Figure 4. It is observed that the maximum vertical displacements are reducing with increase in length of pile. A reduction in vertical displacements of 94% is observed for 28 m long end bearing piles. About 88.8%, 83.6% and 78.2% reduction in vertical displacements reduction are observed for 26 m, 24 m and 22 m long floating piles.

From Figure 6 it is also observed that the maximum horizontal displacements for floating pile supported embankments are reduced but the maximum horizontal displacements for end bearing pile supported embankment are increased. About 1.1% increase in horizontal displacements are observed for 28 m long end bearing pile supported embankment and about 0.04%, 0.25%, 0.53% decrease in horizontal displacements are observed for 26 m, 24 m, 22 m long floating pile supported embankments. This maybe due to the higher amplitude frequency contents of the ground excitations corresponding with increase in pile length (Table 2) and also due to huge reduction in vertical displacements, slight increase in horizontal displacements are seen. From Figures 4 and 5 it is observed that there are considerable deformations in both

Table 2. Natural Frequencies of GRPE's with Fourier amplitudes

GRPE Length of Pile (m)	0	22	24	26	28
Natural Frequency of embankment (Hz)	0.288618	0.29057	0.29126	0.292043	0.29703
Fourier Amplitude	0.02	0.022	0.023	0.026	0.038

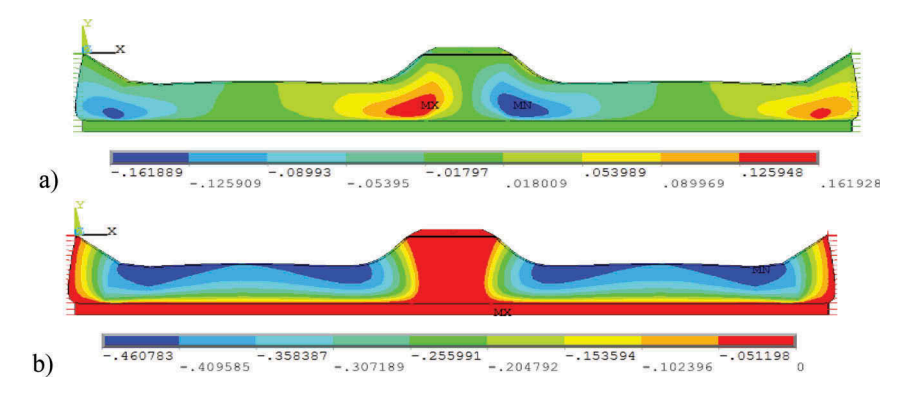


Figure 4. a) Lateral displacements and b) Vertical displacements of end bearing pile supported embankment under self weight

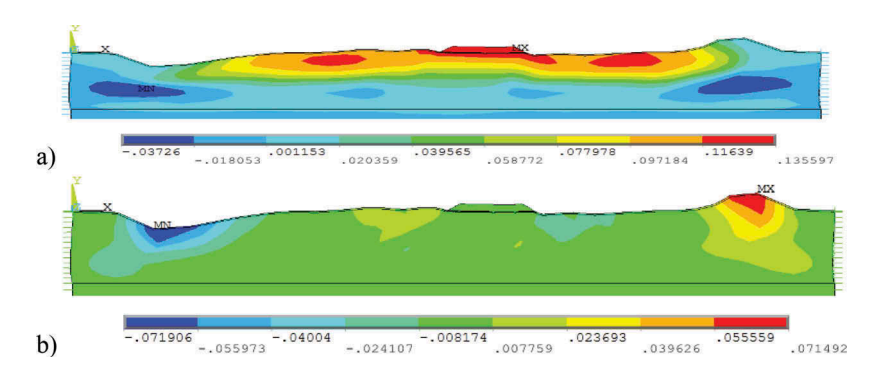


Figure 5. a) Lateral displacements and b) Vertical displacements of end bearing pile supported embankment under El Centro ground motions taken at peak ground accelerations

lateral and vertical directions of the embankment. This indicates that the volumetric strain is the reason for embankment deformations.

3.3 Settlement reduction ratio

Settlement reduction ratio is the ratio between the settlements of reinforced and unreinforced embankments expressed in percentage.

Given by
$$SRR = 1 - \frac{S_{reinf}}{S_{unreinf}}$$
 (3)

Where, S_{reinf} is the settlement of soil with pile and geogrid reinforcement

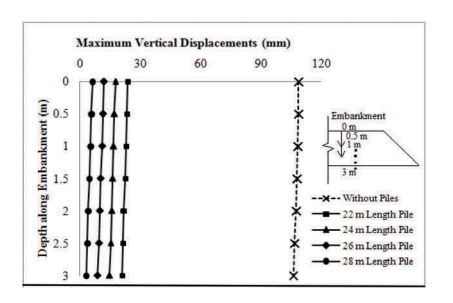
S_{unreinf} is the settlement of soil without pile and geogrid reinforcement.

The settlement reduction ratios (SRR) calculated at crest centre of the embankments under El Centro earthquake excitations are shown in Figure 7.

From Figure 7, SRR is 95% for 28 m long end bearing pile supported embankment and about 85%, 77%, 70% respectively for 26 m, 24 m, 22 m long floating pile supported embankment.

3.4 Differential settlements at crest

The time history of vertical displacements at crest for embankments supported over floating piles and end bearing piles subjected to El Centro earthquake excitations including self weight are shown in Figure 8.



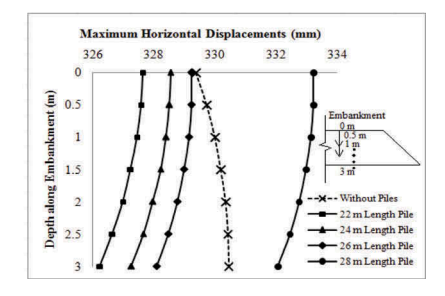


Figure 6. Maximum vertical and horizontal displacements in the embankment under El Centro earthquake excitations

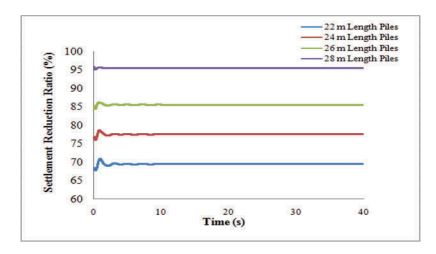


Figure 7. Settlement Reduction ratio at crest centre

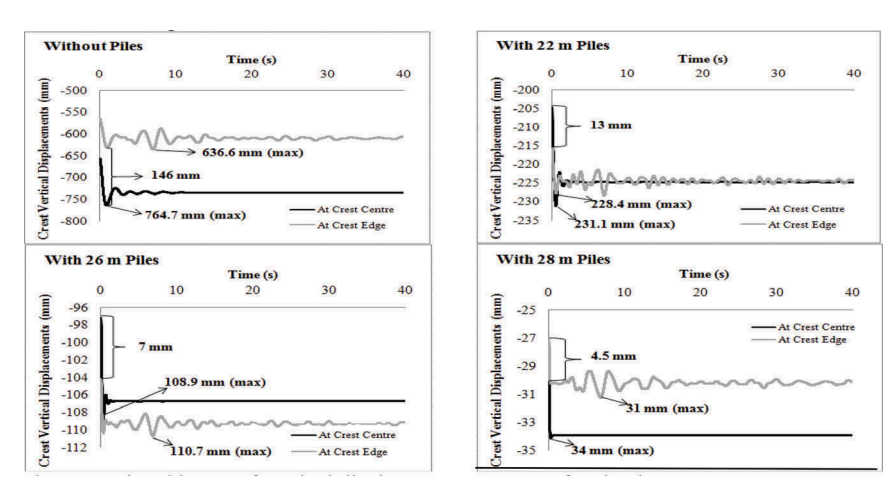


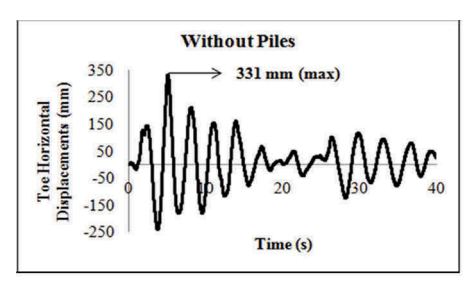
Figure 8. Time history of vertical displacements at crest of embankment

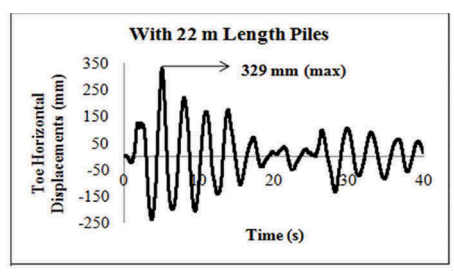
It is observed that, the embankment without pile supports experiences large displacements at crest centre and edge resulting in large differential settlements. But with increase in pile length, these displacements decreases which results in less differential settlements. End bearing pile supported embankment experiences very less vertical displacements at crest and differential settlements.

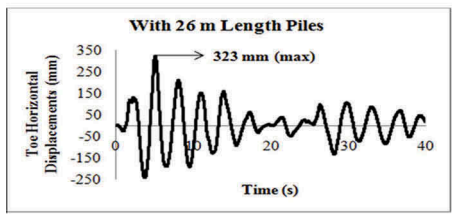
3.5 Horizontal displacements at toe

Figure 9 shows the time history of horizontal displacements at toe of embankments under El Centro earthquake excitations including self weight.

It is observed that the addition of piles reduces the horizontal displacements at toe of all embankments. A reduction of 3% is seen for end bearing pile supported embankment and 0.6%, 2.1%, 2.4% reduction is seen for 22 m, 24 m, 26 m long floating pile supported embankment.







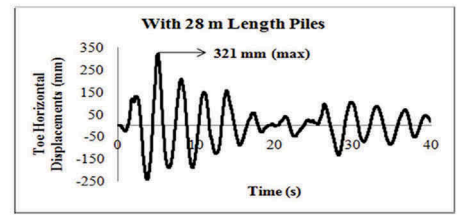


Figure 9. Time history of horizontal displacements at toe of embankments

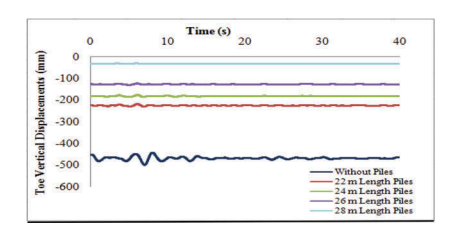


Figure 10. Time history of vertical displacements at toe

3.6 Vertical displacements at toe

Figure 10 shows the time history of vertical displacements at toe of embankments under El Centro earthquake excitations including self weight.

As similar to the vertical displacements at crest, vertical displacements at toe are also reduced with increase in pile length. A reduction of 93% is observed for end bearing pile supported embankment and 73%, 62% and 53% reduction is observed for 26 m, 24 m and 22 m long floating pile supported embankments.

4 CONCLUSIONS

Transient analysis was carried out on 3-dimensional finite element models of GRPE's using El Centro ground motion to study the effect of type and length of pile. Analysis results reveal that, the embankment supported over end bearing piles experienced less vertical displacements at crest centre and edge resulting in less differential settlements at crest. In addition, horizontal and vertical displacements at toe also reduced as compared to the embankment resting over other floating pile combinations considered.

Higher Fourier amplitude corresponding to the natural frequency of the embankments with increased pile length causes almost same horizontal displacements in the embankment supported over floating piles and the embankment without pile supports. Due to the same reasons, the horizontal displacements of end bearing pile supported embankment are also increased.

A SRR of 95% is observed for end bearing pile supported embankment and about 85%, 77% and 70% SRR is observed for 26 m, 24 m, 22 m long floating pile supported embankment.

The addition of piles in a thick soft clay stratum considerably reduces the vertical displacements but need additional stiffening in horizontal direction.

REFERENCES

- Armstrong R. J., Boulanger R. W. & Beaty, M. H. 2013. Liquefaction Effects on Piled Bridge Abutments: CentrifugeTests and Numerical Analyses. J. Geotechnical and Geoenvironmental Eng ASCE 139(3): 433–443.
- Ariyarathne, P. & Liyanapathirana, D. S. 2015. Review of existing design methods for geosynthetic-reinforced pile-supported embankments. J. of Soils and Foundations 55, 17–34.
- BS 8006:2010. Code of Practice for Strengthened/Reinforced Soils and Other Fills. British Standard Institution, UK.
- Briançon, L. & Simon, B. 2011. Performance of pile-supported embankment over soft soil: full-scale experiment. Journal of Geotechnical and Geoenvironmental Engineering 138(4),551–561.
- Bhasi, A. & Rajagopal, K. 2014. Geosynthetic-Reinforced Piled Embankments: Comparisonof Numerical and Analytical Methods. Int. J. Geomech. ASCE. 15 (5):04014074.
- Bhasi, A. & Rajagopal, K. 2015. Numerical study of basal reinforced embankments supported on floating/end bearing piles considering pile-soil interaction. Geotextiles and Geomembranes 43:524–536.
- Carlsson, B. 1987. Reinforced soil, principles for calculation. Terratema AB, Linköping.
- Ghosh, S. & Wilson, E. L. 1969. Analysis of axi-symmetric structures under arbitrary loading (No. 69-10) EERC Report.
- Hewlett, W. J. & Randolph, M. F. 1988. Analysis of piled embankments. Ground Engineering, 21(3), pp.12–18.
- Han, J. & Gabr, M. A. 2002. A numerical study of load transfer mechanisms in geosynthetic reinforced and pile supported embankments over soft soil. J. Geotechnical and Geoenvironmental Engg ASCE 128 (1):44–53.
- Han, G. X., Gong, Q. M. & Zhou, S. H. 2014. Soil arching in a piled embankment under dynamic load. International Journal of Geomechanics 15(6), 04014094.
- IRC:113-2013 Guidelines for the design and construction of geosynthetic reinforced embankments on soft subsoils.
- Jose, B. T., Sridharan, A. & Abraham, B. M. 1988. A study of geotechnical properties of Cochin marine clays. Marine Georesources & Geotechnology 7(3):189–209.
- Kianoush, M. R. & Ghaemmaghami, A. R. 2011. The effect of earthquake frequency content on the seismic behavior of concrete rectangular liquid tanks using the finite element method incorporating soil–structure interaction. Engineering Structures, 33(7):2186–2200.
- Liu, H. L., Charles, W. W. Ng. & Fei, K. 2007. Performance of a Geogrid-Reinforced and Pile-Supported Highway Embankment over Soft Clay: Case Study. J. Geotech. Geoenviron. Engg ASCE 133 (12):1483–1493.
- Liu, K. W., Rowe, R. K., Su, Q., Liu, B. & Yang, Z. 2017. Long-term reinforcement strains for column supported embankments with viscous reinforcement by FEM. Geotextiles and Geomembranes 45(4),307–319.
- Marston, A. & Anderson, A. O. 1913. The theory of loads on pipes in ditches and tests of cement and clay drain tile and sewer pipe. Bulletin No. 31, Iowa Engineering Experiment Station, Ames, Iowa.
- Ousta, R. & Shahrour, I. 2001. Three-dimensional analysis of the seismic behavior of micropiles used in the reinforcement of saturated soil. International Journal for Numerical and Analytical Methods in Geomechanics 25: 183–196.
- Panah, A. K., Yazdi, M. & Ghalandarzadeh, A. 2015. Shaking table tests on soil retaining walls reinforced by polymeric strips. Geotextiles and Geomembranes 43(2),148–161.
- Smith, M. & Filz, G. 2007. Axisymmetric numerical modeling of a unit cell in geosynthetic-reinforced, column-supported embankments. Geosynthetics International 14(1),13–22.
- Shen, P., Xu, C. & Han, J. 2017. Model tests investigating spatial tensile behavior of simulated geosynthetic reinforcement material over rigid supports. Journal of Materials in Civil Engineering 30(2):04017288.
- Syawal Satibi, 2009. Numerical analysis and design criteria of embankments on floating piles. (A PhD Thesis submitted to the University of Stuttgart, Germany).
- Terzaghi, K. 1943. Theoretical Soil Mechanics, New York, John Wiley & Sons, 66.
- Thach, P. N., Liu, H. L. & Kong, G. Q. 2013. Evaluation of PCC pile method in mitigating embankment vibrations from a high-speed train. Journal of Geotechnical and Geoenvironmental Engineering, 139 (12):2225–2228.
- Thach, P. N., Liu, H. L. & Kong, G. Q. 2013. Vibration analysis of pile-supported embankments under high-speed train passage. Soil Dynamics and Earthquake Engineering 55:92–99.

- Wang, L. & Yuan, X. 2005. Decline and dynamic characteristics of micropiles reinforced foundation. Journal of Hydraulic Engineering 12: 1193–1199.
- Wachman, G. S., Biolzi, L. & Labuz, J. F. 2009. Structural behavior of a pile-supported embankment. Journal of geotechnical and geoenvironmental engineering 136(1),26–34.
- Wang, Z. & Mei, G. 2012. Numerical analysis of seismic performance of embankment supported by micropiles. Marine Georesources & Geotechnology, 30(1), 52–62.
- Wang, L., Chen, G. & Chen, S. 2015. Experimental study on seismic response of geogrid reinforced rigid retaining walls with saturated backfill sand. Geotextiles and Geomembranes 43(1):35–45.